14th International Conference on Applications of Statistics and Probability in Civil Engineering, ICASP14
Dublin, Ireland, July 9-13, 2023

Efficient Wiener Path Integral Most Probable Path Determination Based on Extrapolation

Ilias G. Mavromatis
Ph.D. Student, Dept. of Civil Engineering and Engineering Mechanics, Columbia University, New York, USA

Ioannis A. Kougioumtzoglou
Associate Professor, Dept. of Civil Engineering and Engineering Mechanics, Columbia University, New York, USA

ABSTRACT: The Wiener path integral technique for determining the stochastic response of diverse nonlinear dynamical systems relies on a variational formulation that leads to a functional minimization problem. This takes the form of a deterministic boundary value problem (BVP) to be solved for the most probable path, which is used for determining approximately the system response joint transition probability density function (PDF). The BVP corresponds to a specific grid point of the response PDF effective domain. Remarkably, the BVPs corresponding to two neighboring grid points not only share the same equations but, also, the boundary conditions differ only slightly. In this paper, the above unique aspect of the technique is explored further, and it is shown that solution of a BVP and estimation of the response PDF value at a specific grid point can be used for extrapolating and estimating efficiently the PDF values at neighboring points without the need for solving additional BVPs. Notably, the developed approach enhances significantly the computational efficiency of the WPI technique without affecting considerably the exhibited accuracy. An indicative numerical example relating to a Duffing nonlinear oscillator is considered for demonstrating the reliability of the technique. Comparisons with pertinent Monte Carlo simulation data are included as well.

1. INTRODUCTION

The Wiener path integral (WPI) technique, pioneered in the field of stochastic engineering mechanics by Kougioumtzoglou and co-workers (e.g., Kougioumtzoglou and Spanos 2012; Kougioumtzoglou 2017), has exhibited both high accuracy and low computational cost in determining the stochastic response of diverse dynamical systems (e.g., Petromichelakis et al. 2018; Petromichelakis and Kougioumtzoglou 2020; Psaros and Kougioumtzoglou 2020). Further, the WPI technique has proven to be versatile in handling complex non-white/non-Gaussian stochastic excitation modeling (e.g., Psaros et al. 2018), and in treating a wide range of nonlinear/hysteretic systems, even when endowed with fractional derivative elements (e.g., Mavromatis et al. 2023).

The fundamental concept of the WPI technique relates to treating the system response joint transition probability density function (PDF) as a functional integral over the space of all possible paths connecting the initial and the final states of the response vector. Further, the functional integral is evaluated, ordinarily, by resorting to an approximate approach that considers the contribution only of the most probable path. This corresponds to an extremum of the functional integrand and is determined by solving a functional minimization problem that takes the form of a deterministic boundary value problem (BVP). This BVP corresponds to a specific grid point of the response PDF effective domain. Note, however, that for a specific nonlin-

ear system under consideration, the equations of the BVP are independent of the grid point. In fact, only the boundary conditions change with different grid points, whereas the equations of the BVP remain unaltered. Remarkably, the BVPs corresponding to two neighboring grid points not only share the same equations but, also, the boundary conditions differ only slightly. Thus, it is expected that the BVP solutions, i.e., the most probable paths, referring to the two grid points are highly correlated.

In this paper, the above unique aspect of the technique is explored further, and it is shown that solution of a BVP and estimation of the response PDF value at a specific grid point can be used for extrapolating and estimating efficiently the PDF values at neighboring points without the need for solving additional BVPs. Notably, the herein developed approach enhances significantly the computational efficiency of the WPI technique, while exhibiting a satisfactory accuracy degree. An indicative numerical example relating to a Duffing nonlinear oscillator is considered for demonstrating the reliability of the technique. Comparisons with pertinent Monte Carlo simulation (MCS) data are included as well.

2. PRELIMINARIES

2.1. Stochastic differential equations of motion

In the field of stochastic engineering dynamics (e.g., Li and Chen 2009), the equations of motion pertaining to diverse $m-$degree-of-freedom ($m-$DOF) structural and mechanical systems take the form of second-order stochastic differential equations (SDEs) given by

$$\boldsymbol{M}\ddot{\boldsymbol{x}}+\boldsymbol{C}\dot{\boldsymbol{x}}+\boldsymbol{K}\boldsymbol{x}+\boldsymbol{g}\left(\boldsymbol{x},\dot{\boldsymbol{x}},t\right)=\boldsymbol{w}(t), \tag{1}$$

where $\boldsymbol{x}$ denotes the displacement vector process $\left(\boldsymbol{x}=[x_1,\ldots,x_m]^T\right)$; $\boldsymbol{M}$, $\boldsymbol{C}$, $\boldsymbol{K}$ are the $m\times m$ mass, damping and stiffness matrices, respectively; and $\boldsymbol{g}(\cdot)$ represents a nonlinear vector function of arbitrary form that can also account for possible dependence of the state of the system on its history. Further, $\boldsymbol{w}(t)$ is a white noise stochastic vector process with $\mathbb{E}[\boldsymbol{w}(t)]=0$ and $\mathbb{E}[\boldsymbol{w}(t)\boldsymbol{w}^T(t+\tau)]=\boldsymbol{S}_{\boldsymbol{w}}\boldsymbol{\delta}(\tau)$, where $\boldsymbol{S}_{\boldsymbol{w}}\in\mathbb{R}^{m\times m}$ is a non-singular diagonal matrix. Regarding the relation between the Wiener and the white noise processes, a unit intensity white noise process $\boldsymbol{w}(t)$, (i.e., $\boldsymbol{S}_{\boldsymbol{w}}=I$, where I is the identity matrix) can be defined as an infinitesimal jump of the Wiener process, i.e., $\boldsymbol{w}(t)\mathrm{d}t=\mathrm{d}\boldsymbol{W}$. Thus, it is often, informally, written as the time derivative of the Wiener process in the form $\boldsymbol{w}(t)=\frac{\mathrm{d}\boldsymbol{W}}{\mathrm{d}t}$; see also Gardiner (1985) and Øksendal (2003) for a more detailed discussion on the topic.

2.2. Wiener path integral formalism

In comparison to alternative derivations in the literature, which resort to the Chapman-Kolmogorov equation as the starting point, a novel WPI formulation was developed by Mavromatis et al. (2023) that circumvents the Markovian assumption for the system response process. In this regard, nonlinear systems with a history-dependent state, such as hysteretic structures or oscillators endowed with fractional derivative elements, can be treated in a direct manner; that is, without resorting to ad hoc modifications of the WPI technique pertaining, typically, to employing additional auxiliary filter equations and state variables (e.g., Zhang et al. 2023).

Specifically, it has been shown (e.g., Chaichian and Demichev 2001) that the probability of a path corresponding to an $n-$dimensional Wiener vector process with $\boldsymbol{W}(t_0)=\boldsymbol{W}_0$, $\boldsymbol{W}(t_f)=\boldsymbol{W}_f$ and $\Delta\boldsymbol{W}_l=\boldsymbol{W}_{l+1}-\boldsymbol{W}_l$ is given by

$$\begin{aligned}\mathscr{P}[\boldsymbol{W}(t)]=\lim_{\varepsilon\to 0}\Bigg\{&\exp\left(-\frac{1}{2\varepsilon}\sum_{l=0}^{L}\Delta\boldsymbol{W}_l^T\Delta\boldsymbol{W}_l\right)\\&\times\prod_{l=0}^{L}\left[\sqrt{(2\pi\varepsilon)^n}\right]^{-1}\prod_{j=1}^{n}\left[\prod_{l=1}^{L+1}\mathrm{d}W_{j,l}\right]\Bigg\},\end{aligned} \tag{2}$$

where the time domain is discretized into $L+2$ points ε apart (with $L\to\infty$ as $\varepsilon\to 0$), i.e., $t_i=t_0<\cdots<t_{L+1}=t_f$. Further, considering Eq. (2) and accounting for the probabilities of all possible paths that the Wiener process $\boldsymbol{W}$ can follow, the corresponding transition PDF is given as the limit of an $L-$dimensional integral in the form

$$\begin{aligned}&p\left(\boldsymbol{W}_f,t_f|\boldsymbol{W}_i,t_i\right)=\\&\lim_{\varepsilon\to 0}\int_{-\infty}^{\infty}\cdots\int_{-\infty}^{\infty}\exp\left(-\frac{1}{2\varepsilon}\sum_{l=0}^{L}\Delta\boldsymbol{W}_l^T\Delta\boldsymbol{W}_l\right)\\&\qquad\times\prod_{l=0}^{L}\left[\sqrt{(2\pi\varepsilon)^n}\right]^{-1}\prod_{j=1}^{n}\left[\prod_{l=1}^{L+1}\mathrm{d}W_{j,l}\right].\end{aligned} \tag{3}$$

Next, taking into account the relationship between the system response process $\boldsymbol{x}$ and the white noise process $\boldsymbol{w}$ described by Eq. (1), the transition PDF $p(\boldsymbol{x}_f,\dot{\boldsymbol{x}}_f,t_f|\boldsymbol{x}_i,\dot{\boldsymbol{x}}_i,t_i)$ is obtained by applying a functional change of variables to Eq. (3); see Mavromatis et al. (2023) for more details.

In this regard, denoting the set of all paths with initial state $\boldsymbol{x}_i$ at time t_i and final state $\boldsymbol{x}_f$ at time t_f by $\mathscr{C}\{\boldsymbol{x}_f,\dot{\boldsymbol{x}}_f,t_f;\boldsymbol{x}_i,\dot{\boldsymbol{x}}_i,t_i\}$, the joint transition PDF $p(\boldsymbol{x}_f,\dot{\boldsymbol{x}}_f,t_f|\boldsymbol{x}_i,\dot{\boldsymbol{x}}_i,t_i)$ takes the form of a functional integral over $\mathscr{C}\{\boldsymbol{x}_f,\dot{\boldsymbol{x}}_f,t_f;\boldsymbol{x}_i,\dot{\boldsymbol{x}}_i,t_i\}$, i.e.,

$$p(\boldsymbol{x}_f,\dot{\boldsymbol{x}}_f,t_f|\boldsymbol{x}_i,\dot{\boldsymbol{x}}_i,t_i) = \int\limits_{\mathscr{C}\{\boldsymbol{x}_f,\dot{\boldsymbol{x}}_f,t_f;\boldsymbol{x}_i,\dot{\boldsymbol{x}}_i,t_i\}} \exp\left(-S[\boldsymbol{x},\dot{\boldsymbol{x}},\ddot{\boldsymbol{x}}]\right)\mathscr{D}[\boldsymbol{x}(t)], \quad (4)$$

where

$$S[\boldsymbol{x},\dot{\boldsymbol{x}},\ddot{\boldsymbol{x}}] = \int\limits_{t_i}^{t_f} \mathscr{L}[\boldsymbol{x},\dot{\boldsymbol{x}},\ddot{\boldsymbol{x}}]\mathrm{d}t \quad (5)$$

denotes the stochastic action. The Lagrangian functional $\mathscr{L}[\boldsymbol{x},\dot{\boldsymbol{x}},\ddot{\boldsymbol{x}}]$ in Eq. (5) takes the form

$$\mathscr{L}[\boldsymbol{x},\dot{\boldsymbol{x}},\ddot{\boldsymbol{x}}] = \frac{1}{2}\left[\boldsymbol{M}\ddot{\boldsymbol{x}}+\boldsymbol{C}\dot{\boldsymbol{x}}+\boldsymbol{K}\boldsymbol{x}+\boldsymbol{g}\left(\boldsymbol{x},\dot{\boldsymbol{x}},t\right)\right]^T \times \boldsymbol{S}_{\boldsymbol{w}}^{-1}\left[\boldsymbol{M}\ddot{\boldsymbol{x}}+\boldsymbol{C}\dot{\boldsymbol{x}}+\boldsymbol{K}\boldsymbol{x}+\boldsymbol{g}\left(\boldsymbol{x},\dot{\boldsymbol{x}},t\right)\right] \quad (6)$$

and the functional measure $\mathscr{D}[\boldsymbol{x}(t)]$ is given by

$$\mathscr{D}[\boldsymbol{x}(t)] = \prod_{j=1}^{m}\mathscr{D}[\boldsymbol{x}_j(t)] = \prod_{j=1}^{m}\prod_{t=t_i}^{t_f}\frac{\mathrm{d}x_j(t)}{\sqrt{2\pi\left(\det\left[\boldsymbol{M}^{-1}\boldsymbol{S}_{\boldsymbol{w}}\left(\boldsymbol{M}^{-1}\right)^T\right]\right)^{1/m}\mathrm{d}t}}. \quad (7)$$

2.3. Most probable path approximation

It is remarked that the analytical evaluation of the WPI of Eq. (4) is, in general, an impossible task. Thus, alternative approaches are typically pursued in the literature for evaluating approximately Eq. (4), such as the most probable path approach (e.g., Chaichian and Demichev 2001). Note that the most probable path approximation has exhibited a quite high degree of accuracy in various diverse engineering mechanics applications (e.g., Kougioumtzoglou 2017; Petromichelakis et al. 2018).

Specifically, the largest contribution to the functional integral of Eq. (4) relates to the trajectory $\boldsymbol{x}_c(t)$ for which the stochastic action of Eq. (5) becomes as small as possible. This leads to the variational (functional minimization) problem

$$\underset{\mathscr{C}\{\boldsymbol{x}_i,\dot{\boldsymbol{x}}_i,t_i;\boldsymbol{x}_f,\dot{\boldsymbol{x}}_f,t_f\}}{\text{minimize}} \quad S[\boldsymbol{x},\dot{\boldsymbol{x}},\ddot{\boldsymbol{x}}]. \quad (8)$$

Following the solution of Eq. (8) and determination of $\boldsymbol{x}_c(t)$, the functional integral of Eq. (4) is evaluated approximately as

$$p(\boldsymbol{x}_f,\dot{\boldsymbol{x}}_f,t_f|\boldsymbol{x}_i,\dot{\boldsymbol{x}}_i,t_i) = C\exp\left(-S[\boldsymbol{x}_c,\dot{\boldsymbol{x}}_c,\ddot{\boldsymbol{x}}_c]\right), \quad (9)$$

where C is a constant to be determined by the normalization condition

$$\int\limits_{-\infty}^{\infty}\int\limits_{-\infty}^{\infty} p(\boldsymbol{x}_f,\dot{\boldsymbol{x}}_f,t_f|\boldsymbol{x}_i,\dot{\boldsymbol{x}}_i,t_i)\mathrm{d}\boldsymbol{x}_f\mathrm{d}\dot{\boldsymbol{x}}_f = 1. \quad (10)$$

Various methodologies can be employed for treating the optimization problem of Eq. (8) and for determining $\boldsymbol{x}_c(t)$. These range from standard Rayleigh-Ritz type numerical solution schemes (e.g., Kougioumtzoglou 2017; Petromichelakis et al. 2020) to more recently developed techniques relying on computational algebraic geometry tools (Petromichelakis et al. 2021).

Alternatively, the most probable path $\boldsymbol{x}_c(t)$, being an extremal of $S[\boldsymbol{x}_c,\dot{\boldsymbol{x}}_c,\ddot{\boldsymbol{x}}_c]$, can be determined by resorting to calculus of variations (e.g. Gelfand and Fomin 1963) and enforcing the necessary condition that the first variation vanishes, i.e., $\delta S[\boldsymbol{x}_c,\dot{\boldsymbol{x}}_c,\ddot{\boldsymbol{x}}_c] = 0$. This yields the corresponding system of Euler-Lagrange equations for $j = 1,\ldots,m$

$$\frac{\partial\mathscr{L}}{\partial x_j} - \frac{\mathrm{d}}{\mathrm{d}t}\frac{\partial\mathscr{L}}{\partial\dot{x}_j} + \frac{\mathrm{d}^2}{\mathrm{d}t^2}\frac{\partial\mathscr{L}}{\partial\ddot{x}_j} = 0, \quad (11)$$

in conjunction with the boundary conditions

$$\begin{aligned} x_j(t_i) &= x_{j,i},\\ \dot{x}_j(t_i) &= \dot{x}_{j,i},\\ x_j(t_f) &= x_{j,f},\\ \dot{x}_j(t_f) &= \dot{x}_{j,f}. \end{aligned} \quad (12)$$

3. MATHEMATICAL FORMULATION

As discussed in section 2.3, the most probable path $\boldsymbol{x}_c(t)$, which is used for determining approximately the system response joint transition PDF via Eq. (9), is computed by solving a functional minimization problem that takes the form of a deterministic BVP described by Eqs. (11-12). This BVP corresponds to a specific grid point of the response PDF effective domain. In fact, for a given time instant t_f, a standard brute-force numerical implementation of the technique entails the discretization of the PDF effective domain into N^{2m} points, where N is the number of points in each dimension. Next, the evaluation of the PDF is performed pointwise on the discretized lattice. In other words, N^{2m} BVPs in the form of Eqs. (11-12) need to be solved numerically, yielding an exponential increase of the computational cost with the dimension m of the system.

To circumvent the aforementioned challenge, attention is directed in the following to the fact that, for a specific nonlinear system under consideration, the equations of the BVP are independent of the grid point. In fact, only the boundary conditions change with different grid points, whereas the equations of the BVP remain unaltered. Remarkably, the BVPs corresponding to two neighboring grid points not only share the same equations but, also, the boundary conditions differ only slightly. Thus, it is expected that the BVP solutions, i.e., the most probable paths referring to the two grid points, are highly correlated. This unique aspect of the technique is explored further in the ensuing analysis, and the BVP solution at a given point is determined by extrapolating the BVP solution at a neighboring point.

Specifically, consider a point $(\boldsymbol{x}'_f, \dot{\boldsymbol{x}}'_f)$ in the response PDF domain expressed as $(\boldsymbol{x}'_f, \dot{\boldsymbol{x}}'_f) = (\boldsymbol{x}_f + \Delta\boldsymbol{x}_f, \dot{\boldsymbol{x}}_f + \Delta\dot{\boldsymbol{x}}_f)$, where $(\boldsymbol{x}_f, \dot{\boldsymbol{x}}_f)$ denotes the point corresponding to the final conditions used in the BVP of Eqs. (11-12). Accordingly, the most probable path corresponding to initial conditions $(\boldsymbol{x}_i, \dot{\boldsymbol{x}}_i)$ and final conditions $(\boldsymbol{x}'_f, \dot{\boldsymbol{x}}'_f)$ is expressed as $\boldsymbol{x}'_c = \boldsymbol{x}_c + \Delta\boldsymbol{x}$, where $\Delta\boldsymbol{x}$ denotes a path to be determined. Next, substituting $\boldsymbol{x}'_c = \boldsymbol{x}_c + \Delta\boldsymbol{x}$ into the Lagrangian functional of Eq. (6) yields

$$\begin{aligned}\mathscr{L}[\boldsymbol{x}'_c, \dot{\boldsymbol{x}}'_c, \ddot{\boldsymbol{x}}'_c] = \frac{1}{2}\,&[\boldsymbol{M}(\ddot{\boldsymbol{x}}_c + \Delta\ddot{\boldsymbol{x}}) + \boldsymbol{C}(\dot{\boldsymbol{x}}_c + \Delta\dot{\boldsymbol{x}}) \\ &+ \boldsymbol{K}(\boldsymbol{x}_c + \Delta\boldsymbol{x}) + \boldsymbol{g}\,(\boldsymbol{x}_c + \Delta\boldsymbol{x}, \dot{\boldsymbol{x}}_c + \Delta\dot{\boldsymbol{x}}, t)]^T \\ &\times \boldsymbol{S}_{\boldsymbol{w}}^{-1}\,[\boldsymbol{M}(\ddot{\boldsymbol{x}}_c + \Delta\ddot{\boldsymbol{x}}) + \boldsymbol{C}(\dot{\boldsymbol{x}}_c + \Delta\dot{\boldsymbol{x}}) \\ &+ \boldsymbol{K}(\boldsymbol{x}_c + \Delta\boldsymbol{x}) + \boldsymbol{g}\,(\boldsymbol{x}_c + \Delta\boldsymbol{x}, \dot{\boldsymbol{x}}_c + \Delta\dot{\boldsymbol{x}}, t)]\,.\end{aligned} \tag{13}$$

Eq. (13) is cast, equivalently, in the form

$$\begin{aligned}\mathscr{L}[\boldsymbol{x}'_c, \dot{\boldsymbol{x}}'_c, \ddot{\boldsymbol{x}}'_c] = \frac{1}{2}\,\Big[&(\boldsymbol{A}(\boldsymbol{x}_c, \Delta\boldsymbol{x}) + \boldsymbol{B}_{\text{lin}}(\Delta\boldsymbol{x}))^T \\ &\times \boldsymbol{S}_{\boldsymbol{w}}^{-1}\,(\boldsymbol{A}(\boldsymbol{x}_c, \Delta\boldsymbol{x}) + \boldsymbol{B}_{\text{lin}}(\Delta\boldsymbol{x}))\Big]\,,\end{aligned} \tag{14}$$

where

$$\begin{aligned}&\boldsymbol{A}(\boldsymbol{x}_c, \Delta\boldsymbol{x}) = \\ &\quad \boldsymbol{M}\ddot{\boldsymbol{x}}_c + \boldsymbol{C}\dot{\boldsymbol{x}}_c + \boldsymbol{K}\boldsymbol{x}_c + \boldsymbol{g}\,(\boldsymbol{x}_c + \Delta\boldsymbol{x}, \dot{\boldsymbol{x}}_c + \Delta\dot{\boldsymbol{x}}, t)\,,\end{aligned} \tag{15}$$

and

$$\boldsymbol{B}_{\text{lin}}(\Delta\boldsymbol{x}) = \boldsymbol{M}\Delta\ddot{\boldsymbol{x}} + \boldsymbol{C}\Delta\dot{\boldsymbol{x}} + \boldsymbol{K}\Delta\boldsymbol{x}. \tag{16}$$

In the following, it is assumed that the two points, $(\boldsymbol{x}'_f, \dot{\boldsymbol{x}}'_f)$ and $(\boldsymbol{x}_f, \dot{\boldsymbol{x}}_f)$, are sufficiently close in the PDF domain, and thus their difference $(\Delta\boldsymbol{x}_f, \Delta\dot{\boldsymbol{x}}_f)$ is relatively small. Also, note that the two BVPs corresponding to $(\boldsymbol{x}'_f, \dot{\boldsymbol{x}}'_f)$ and $(\boldsymbol{x}_f, \dot{\boldsymbol{x}}_f)$ and governed by Eqs. (11-12) have identical equations with only slightly different boundary conditions. Thus, it is reasonable to assume that the term $\Delta\boldsymbol{x}$ is also relatively small. In other words, the BVP solutions, i.e., the two most probable paths $\boldsymbol{x}'_c$ and $\boldsymbol{x}_c$, corresponding to $(\boldsymbol{x}'_f, \dot{\boldsymbol{x}}'_f)$ and $(\boldsymbol{x}_f, \dot{\boldsymbol{x}}_f)$ respectively, are expected to differ only slightly. In this regard, adopting next the approximation $\boldsymbol{g}\,(\boldsymbol{x}_c + \Delta\boldsymbol{x}, \dot{\boldsymbol{x}}_c + \Delta\dot{\boldsymbol{x}}, t) = \boldsymbol{g}\,(\boldsymbol{x}_c, \dot{\boldsymbol{x}}_c, t)$ and employing the Cauchy-Schwarz inequality (e.g., Steele 2004), Eq. (14) is approximated by

$$\begin{aligned}\mathscr{L}_{\text{approx}}[\boldsymbol{x}'_c, \dot{\boldsymbol{x}}'_c, \ddot{\boldsymbol{x}}'_c] = &\frac{1}{2}\boldsymbol{A}^T(\boldsymbol{x}_c)\boldsymbol{S}_{\boldsymbol{w}}^{-1}\boldsymbol{A}(\boldsymbol{x}_c) + \\ &+ \frac{1}{2}\boldsymbol{B}_{\text{lin}}^T(\Delta\boldsymbol{x})\boldsymbol{S}_{\boldsymbol{w}}^{-1}\boldsymbol{B}_{\text{lin}}(\Delta\boldsymbol{x}).\end{aligned} \tag{17}$$

Further, considering the form of the Lagrangian of Eq. (6), Eq. (17) can be written, equivalently, as

$$\begin{aligned}&\mathscr{L}_{\text{approx}}[\boldsymbol{x}'_c, \dot{\boldsymbol{x}}'_c, \ddot{\boldsymbol{x}}'_c] = \\ &\qquad \mathscr{L}[\boldsymbol{x}_c, \dot{\boldsymbol{x}}_c, \ddot{\boldsymbol{x}}_c] + \mathscr{L}_{\text{lin}}(\Delta\boldsymbol{x}, \Delta\dot{\boldsymbol{x}}, \Delta\ddot{\boldsymbol{x}}),\end{aligned} \tag{18}$$

where

$$\mathscr{L}_{\text{lin}}(\Delta\boldsymbol{x},\Delta\dot{\boldsymbol{x}},\Delta\ddot{\boldsymbol{x}}) = \frac{1}{2}\boldsymbol{B}_{\text{lin}}^{T}(\Delta\boldsymbol{x})\boldsymbol{S}_{\boldsymbol{w}}^{-1}\boldsymbol{B}_{\text{lin}}(\Delta\boldsymbol{x}). \quad (19)$$

Next, substituting Eq. (18) into Eq. (5) yields

$$\begin{aligned} S_{\text{approx}}[\boldsymbol{x}_c',\dot{\boldsymbol{x}}_c',\ddot{\boldsymbol{x}}_c'] = \\ S[\boldsymbol{x}_c,\dot{\boldsymbol{x}}_c,\ddot{\boldsymbol{x}}_c] + S_{\text{lin}}[\Delta\boldsymbol{x},\Delta\dot{\boldsymbol{x}},\Delta\ddot{\boldsymbol{x}}], \end{aligned} \quad (20)$$

where $S_{\text{lin}}[\Delta\boldsymbol{x},\Delta\dot{\boldsymbol{x}},\Delta\ddot{\boldsymbol{x}}]$ is the stochastic action corresponding to the Lagrangian of Eq. (19). Further, following section 2.3, $\boldsymbol{x}_c'$ is determined by solving the functional minimization problem

$$\underset{\mathscr{C}\{\boldsymbol{x}_i',\dot{\boldsymbol{x}}_i',t_i;\boldsymbol{x}_f',\dot{\boldsymbol{x}}_f',t_f\}}{\text{minimize}} \quad S_{\text{approx}}[\boldsymbol{x}_c',\dot{\boldsymbol{x}}_c',\ddot{\boldsymbol{x}}_c']. \quad (21)$$

Note, however, that in Eq. (20), the first term depends only on $\boldsymbol{x}_c$, which is considered to be a known function obtained by solving the BVP of Eqs. (11-12) corresponding to point $(\boldsymbol{x}_f,\dot{\boldsymbol{x}}_f)$. In this regard, $S[\boldsymbol{x}_c,\dot{\boldsymbol{x}}_c,\ddot{\boldsymbol{x}}_c]$ is treated as a constant in the functional minimization problem of Eq. (21), and thus, Eq. (21) degenerates to

$$\underset{\mathscr{C}\{0,0,t_i;\Delta\boldsymbol{x}_f,\Delta\dot{\boldsymbol{x}}_f,t_f\}}{\text{minimize}} \quad S_{\text{lin}}[\Delta\boldsymbol{x},\Delta\dot{\boldsymbol{x}},\Delta\ddot{\boldsymbol{x}}]. \quad (22)$$

Further, the Euler-Lagrange Eqs. (11-12) corresponding to Eq. (22) take the form

$$\frac{\partial\mathscr{L}_{\text{lin}}}{\partial\Delta x_j} - \frac{\mathrm{d}}{\mathrm{d}t}\frac{\partial\mathscr{L}_{\text{lin}}}{\partial\Delta\dot{x}_j} + \frac{\mathrm{d}^2}{\mathrm{d}t^2}\frac{\partial\mathscr{L}_{\text{lin}}}{\partial\Delta\ddot{x}_j} = 0, \quad (23)$$

with the boundary conditions

$$\begin{aligned} &\Delta x_j(t_i) = 0, \\ &\Delta\dot{x}_j(t_i) = 0, \\ &\Delta x_j(t_f) = \Delta x_{j,f}, \\ &\Delta\dot{x}_j(t_f) = \Delta\dot{x}_{j,f}. \end{aligned} \quad (24)$$

Remarkably, the form of the optimization problem of Eq. (22), or of the associated Euler-Lagrange Eqs. (23-24), is identical to that corresponding to a linear oscillator under Gaussian white noise (Psaros et al. 2020). In fact, as shown in Psaros et al. (2020), Eqs.(23-24) are amenable to analytical solution treatment yielding

$$\Delta\boldsymbol{x} = C_1\boldsymbol{v}_1 e^{\lambda_1 t} + C_2\boldsymbol{v}_2 e^{\lambda_2 t} + \cdots + C_{4m}\boldsymbol{v}_{4m}e^{\lambda_{4m}t}, \quad (25)$$

where $[C_1,C_2,\ldots,C_{4m}]^T$ is a vector containing $4m$ coefficients to be determined by enforcing the boundary conditions of Eq. (24) and $\{\boldsymbol{v}_1,\boldsymbol{v}_2,\ldots,\boldsymbol{v}_{4m}\}$, $\{\lambda_1,\lambda_2,\ldots,\lambda_{4m}\}$ are the eigenvectors and eigenvalues, respectively, to be determined by solving the eigenvalue problem

$$(\boldsymbol{M}\lambda^2 - \boldsymbol{C}\lambda + \boldsymbol{K})^T\boldsymbol{S}_{\boldsymbol{w}}^{-1}(\boldsymbol{M}\lambda^2 + \boldsymbol{C}\lambda + \boldsymbol{K})\boldsymbol{v} = 0. \quad (26)$$

For more details on the derivation and the exact analytical expressions of the coefficients and of the eigenvalues and eigenvectors in Eq. (25), the interested reader is referred to Psaros et al. (2020). Further, Eq. (25) is substituted into the Lagrangian of Eq. (13) and the joint response PDF $p(\boldsymbol{x}_f',\dot{\boldsymbol{x}}_f',t_f|\boldsymbol{x}_i,\dot{\boldsymbol{x}}_i,t_i)$ given by Eq. (9) becomes

$$p(\boldsymbol{x}_f',\dot{\boldsymbol{x}}_f',t_f|\boldsymbol{x}_i,\dot{\boldsymbol{x}}_i,t_i) = C'\exp\left(-S[\boldsymbol{x}_c',\dot{\boldsymbol{x}}_c',\ddot{\boldsymbol{x}}_c']\right), \quad (27)$$

where C' is a normalization constant given by Eq. (10).

Overall, it is readily seen that the PDF value at a point $(\boldsymbol{x}_f',\dot{\boldsymbol{x}}_f')$ sufficiently close to point $(\boldsymbol{x}_f,\dot{\boldsymbol{x}}_f)$ can be approximated by Eq. (27). From a computational cost perspective, it is highlighted that once the most probable path $\boldsymbol{x}_c(t)$ corresponding to the original point $(\boldsymbol{x}_f,\dot{\boldsymbol{x}}_f)$ has been determined, the herein developed extrapolation technique requires zero additional computational effort for obtaining the PDF values at neighboring points $(\boldsymbol{x}_f',\dot{\boldsymbol{x}}_f')$. Indeed, Eq. (27) depends on $\boldsymbol{x}_c' = \boldsymbol{x}_c + \Delta\boldsymbol{x}$, where $\Delta\boldsymbol{x}$ is calculated analytically and is given by Eq. (25) in closed-form.

4. NUMERICAL EXAMPLE

Consider a single-DOF Duffing nonlinear oscillator governed by Eq. (1) with $\boldsymbol{g}(x,\dot{x},t) = \varepsilon x^3$ and parameter values $m = 1, c = 0.25, k = 1, \varepsilon = 0.3, S_0 = 0.0637$. For an arbitrarily selected time instant $t_f = 4s$, the joint response PDF $p(x_f,\dot{x}_f,t_f|0,0,0)$ is evaluated at $N^2 = 11^2$ points based on the WPI technique. Next, the herein developed extrapolation approach is employed for estimating the PDF values at a grid of $N^2 = 201^2$ points spanning the entire PDF effective domain. The results are plotted in Figure 1 and compared with a brute-force implementation of the WPI tech-

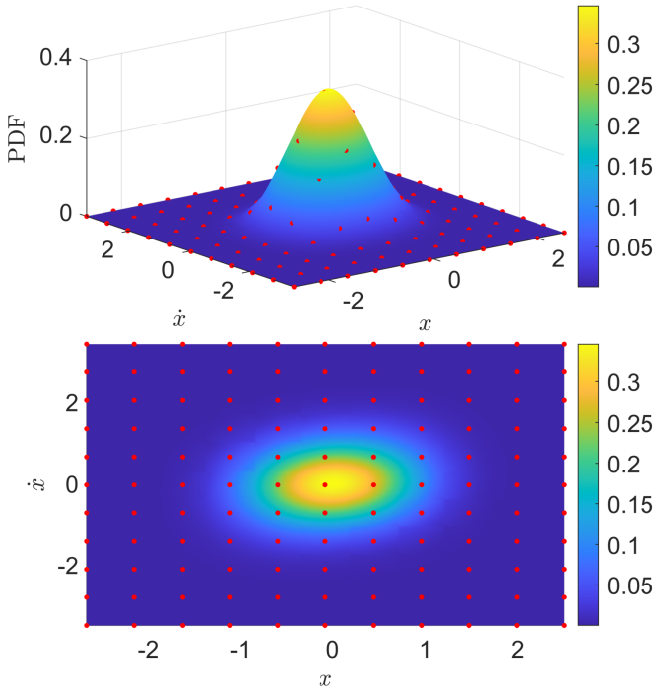

Figure 1: Joint response PDF at an indicative time instant $t_f = 4s$ corresponding to a single-DOF Duffing nonlinear oscillator: WPI technique - Original grid of $N = 11^2$ points (red dots) and extrapolation to 201^2 points over the PDF domain.

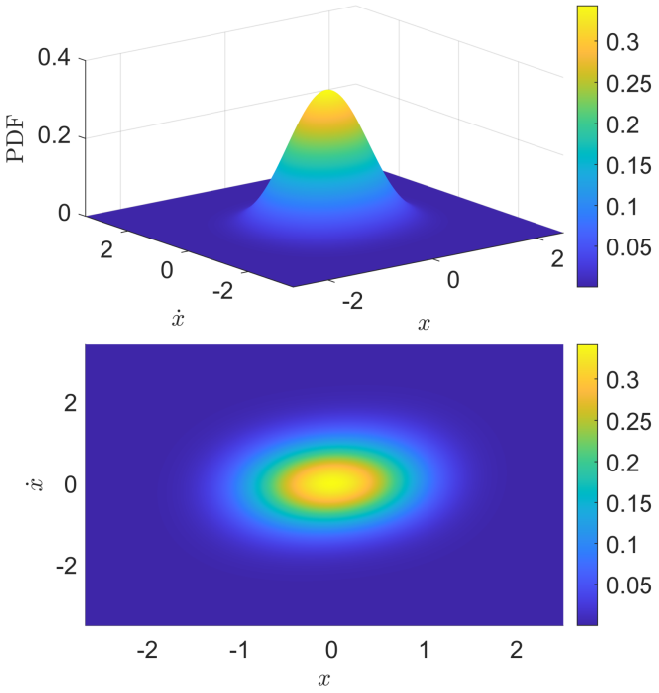

Figure 2: Joint response PDF at an indicative time instant $t_f = 4s$ corresponding to a single-DOF Duffing nonlinear oscillator: WPI technique - Original grid of $N = 201^2$ points over the PDF domain.

nique in Figure 2, where the PDF values are determined, directly, by solving $N^2 = 201^2$ functional minimization problems of the form Eq. (8). It is seen that the proposed extrapolation technique reduces, drastically, the associated computational cost without compromising considerably the overall accuracy. Further, MCS-based estimates (100,000 realizations) are shown in Figure 3, demonstrating the high degree of accuracy exhibited by the WPI technique.

Furthermore, in Figure 4 the y-axis shows the mean square error of the PDF estimates compared with an MCS-based solution employing 100,000 realizations. The x-axis shows the computation time required for obtaining the PDF estimates. Clearly, for a given degree of accuracy, the proposed extrapolation approach is several orders of magnitude more efficient than both a brute-force implementation of the WPI technique and a standard MCS solution scheme.

5. Concluding Remarks

A novel extrapolation approach has been developed in this paper that drastically reduces the computational cost associated with the WPI technique without considerably affecting the exhibited accuracy. Specifically, the WPI technique for determining the stochastic response of diverse nonlinear dynamical systems relies on a variational formulation that leads to a functional minimization problem. This takes the form of a deterministic BVP to be solved for the most probable path, which is used for determining approximately the system response joint transition PDF. The BVP corresponds to a specific grid point of the response PDF effective domain. Remarkably, the BVPs corresponding to two neighboring grid points not only share the same equations but, also, the boundary conditions differ only slightly. In this paper, the above unique aspect of the technique has been exploited, and it has been shown that solution of a BVP and estimation of the response PDF value at a specific grid point can be used for extrapolating and estimat-

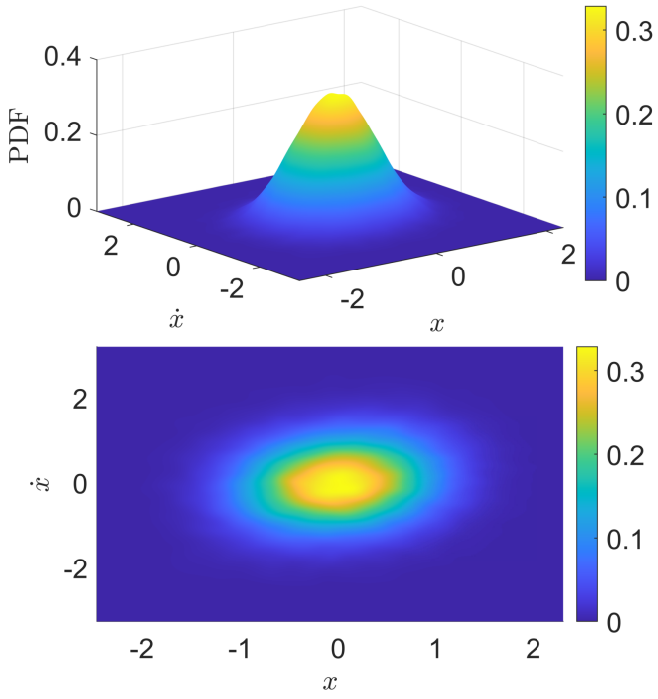

Figure 3: Joint response PDF at an indicative time instant $t_f = 4s$ corresponding to a single-DOF Duffing nonlinear oscillator: MCS data (100,000 realizations).

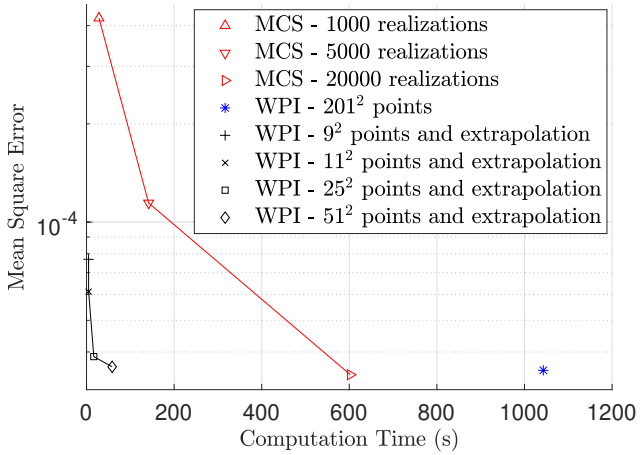

Figure 4: Comparisons between standard MCS, brute-force implementation of the WPI technique, and efficient WPI technique based on extrapolation in terms of accuracy and computational cost: mean square error and associated computation time for estimating the joint response PDF at an indicative time instant $t_f = 4s$ corresponding to a single-DOF Duffing nonlinear oscillator.

ing efficiently the PDF values at neighboring points without the need for solving additional BVPs. Notably, the developed approach enhances considerably the computational efficiency of the WPI technique without compromising significantly the exhibited accuracy. A Duffing nonlinear oscillator has been considered as an indicative example, whereas comparisons with pertinent MCS data have demonstrated the reliability of the technique.

6. References

Chaichian, M. and Demichev, A. (2001). *Path Integrals in Physics*, Vol. 1. IOP Publishing Ltd.

Gardiner, C. (1985). *Handbook of Stochastic Methods for Physics, Chemistry, and the Natural Sciences*. Springer-Verlag, third edition.

Gelfand, I. M. and Fomin, S. V. (1963). *The calculus of variations*. Prentice Hall.

Kougioumtzoglou, I. A. (2017). "A Wiener path integral solution treatment and effective material properties of a class of one-dimensional stochastic mechanics problems." *Journal of Engineering Mechanics*, 143(6), 1–12.

Kougioumtzoglou, I. A. and Spanos, P. D. (2012). "An analytical Wiener path integral technique for non-stationary response determination of nonlinear oscillators." *Probabilistic Engineering Mechanics*, 28, 125–131.

Li, J. and Chen, J. (2009). *Stochastic Dynamics of Structures*. John Wiley & Sons, Ltd, Chichester, UK.

Mavromatis, I. G., Psaros, A. F., and Kougioumtzoglou, I. A. (2023). "A Wiener Path Integral Formalism for Treating Nonlinear Systems with Non-Markovian Response Processes." *Journal of Engineering Mechanics*, 149(1), 1–11.

Øksendal, B. (2003). *Stochastic Differential Equations*. Universitext. Springer, Berlin, Heidelberg, fifth edition.

Petromichelakis, I., Bosse, R. M., Kougioumtzoglou, I. A., and Beck, A. T. (2021). "Wiener path integral most probable path determination: A computational algebraic geometry solution treatment." *Mechanical Systems and Signal Processing*, 153, 107534.

Petromichelakis, I. and Kougioumtzoglou, I. A. (2020). "Addressing the curse of dimensionality in stochastic dynamics: A Wiener path integral variational formulation with free boundaries." *Proceedings of the Royal Society A: Mathematical, Physical and Engineering Sciences*, 476(2243).

Petromichelakis, I., Psaros, A. F., and Kougioumtzoglou, I. A. (2018). "Stochastic response determination and optimization of a class of nonlinear electromechanical energy harvesters: A Wiener path integral approach." *Probabilistic Engineering Mechanics*, 53, 116–125.

Petromichelakis, I., Psaros, A. F., and Kougioumtzoglou, I. A. (2020). "Stochastic response determination of nonlinear structural systems with singular diffusion matrices: A Wiener path integral variational formulation with constraints." *Probabilistic Engineering Mechanics*, 60, 103044.

Psaros, A. F., Brudastova, O., Malara, G., and Kougioumtzoglou, I. A. (2018). "Wiener Path Integral based response determination of nonlinear systems subject to non-white, non-Gaussian, and non-stationary stochastic excitation." *Journal of Sound and Vibration*, 433, 314–333.

Psaros, A. F. and Kougioumtzoglou, I. A. (2020). "Functional Series Expansions and Quadratic Approximations for Enhancing the Accuracy of the Wiener Path Integral Technique." *Journal of Engineering Mechanics*, 146(7), 04020065.

Psaros, A. F., Zhao, Y., and Kougioumtzoglou, I. A. (2020). "An exact closed-form solution for linear multi-degree-of-freedom systems under Gaussian white noise via the Wiener path integral technique." *Probabilistic Engineering Mechanics*, 60, 103040.

Steele, J. M. (2004). *The Cauchy-Schwarz Master Class: An Introduction to the Art of Mathematical Inequalities*. Cambridge University Press.

Zhang, Y., Kougioumtzoglou, I. A., and Kong, F. (2023). "A Wiener path integral technique for determining the stochastic response of nonlinear oscillators with fractional derivative elements: A constrained variational formulation with free boundaries." *Probabilistic Engineering Mechanics*, 71, 103410.